

## ONLINE SUPPLEMENTARY MATERIALS

### Serendipitous alkylation of a Plk1 ligand uncovers a new binding channel

Fa Liu,<sup>1,5</sup> Jung-Eun Park,<sup>2,5</sup> Wen-Jian Qian,<sup>1</sup> Dan Lim,<sup>3</sup> Martin Gräber,<sup>4</sup> Thorsten Berg,<sup>4</sup> Michael B. Yaffe,<sup>3</sup> Kyung S. Lee<sup>2\*</sup> and Terrence R. Burke, Jr.<sup>1\*</sup>

<sup>1</sup>*Chemical Biology Laboratory, Molecular Discovery Program, Center for Cancer Research, National Cancer Institute-Frederick, Frederick, MD 21702, U. S. A., and* <sup>2</sup>*Laboratory of Metabolism, Center for Cancer Research, National Cancer Institute, National Institutes of Health, Bethesda, MD 20892, U. S. A. and* <sup>3</sup>*Department of Biology and Biological Engineering, Center for Cancer Research, Massachusetts Institute of Technology, Cambridge, MA 02139, U. S. A. and* <sup>4</sup>*Institute of Organic Chemistry, University of Leipzig, Leipzig, Germany*

\*Corresponding authors:

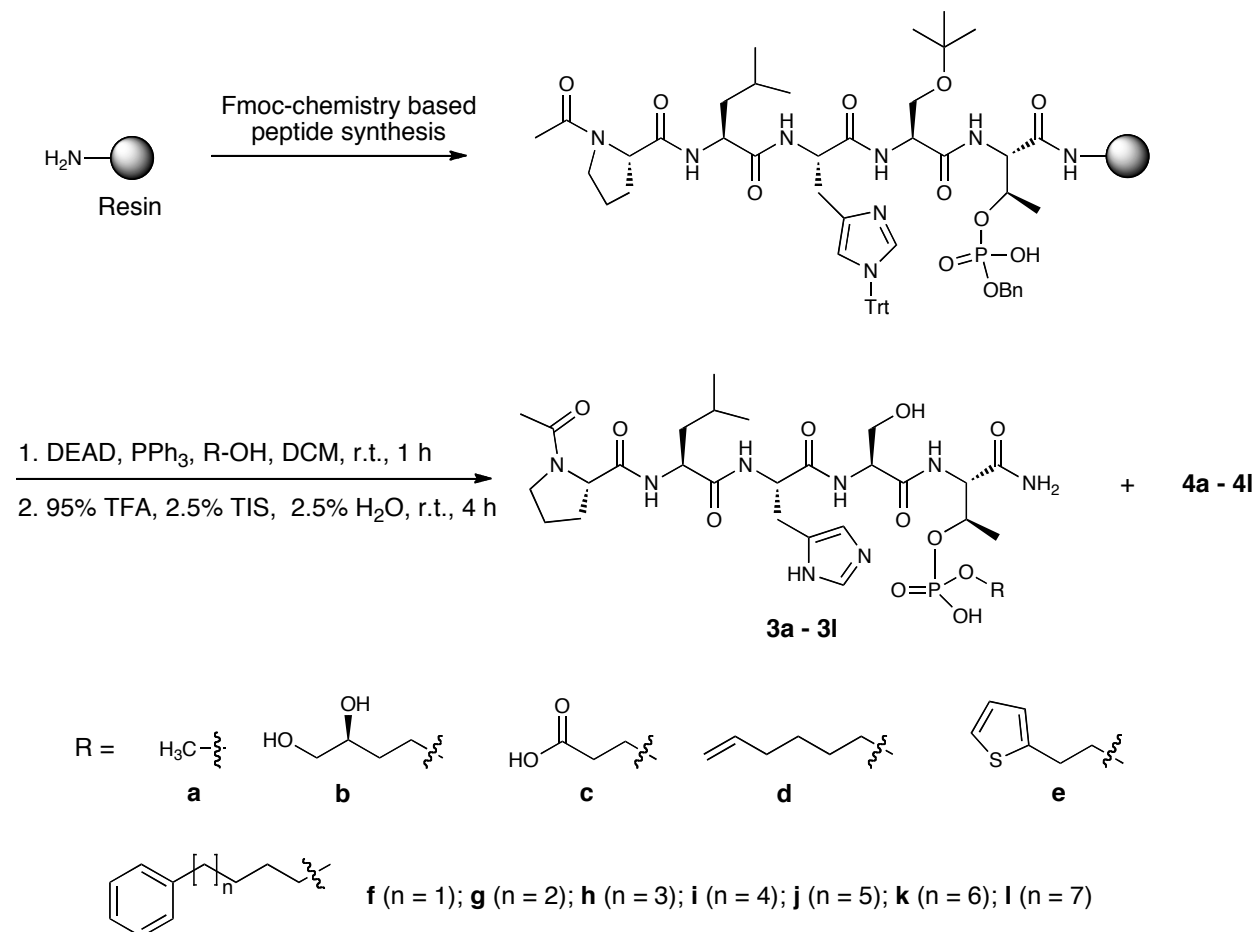
Terrence R. Burke, Jr., Ph.D.  
National Cancer Institute  
National Institutes of Health  
Building 376 Boyles St., NCI-Frederick  
Frederick, MD 21702  
U. S. A.  
Phone: (301) 846-5906; Fax: (301) 846-6033  
E-mail: [tburke@helix.nih.gov](mailto:tburke@helix.nih.gov)

And

Kyung S. Lee, Ph.D.  
National Cancer Institute  
National Institutes of Health  
9000 Rockville Pike  
Building 37, Room 3118  
Bethesda, MD 20892  
U. S. A.  
Phone: (301) 496-9635, Fax: (301) 496-8419  
E-mail: [kyunglee@mail.nih.gov](mailto:kyunglee@mail.nih.gov)

<sup>5</sup>These authors contributed equally to this work.

## SUPPLEMENTARY METHODS



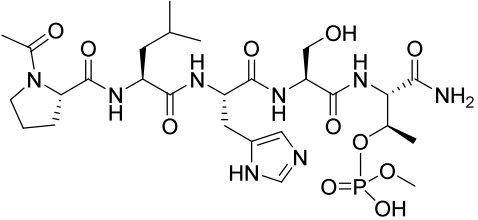
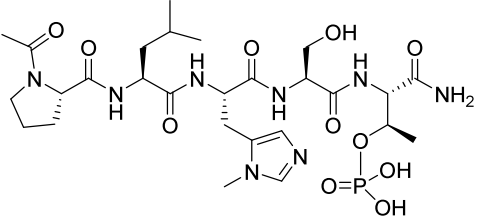
**Supplementary Figure 1.** Solid-phase synthesis of peptides **3** and **4**.

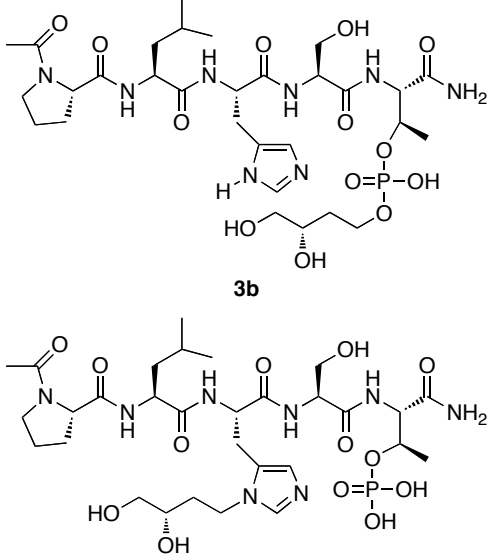
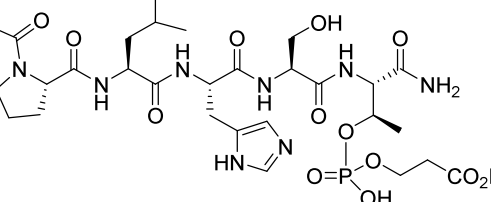
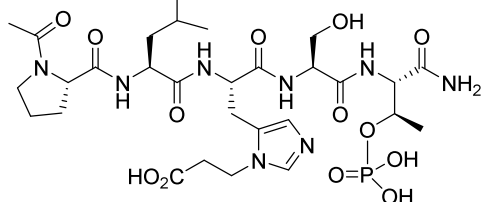
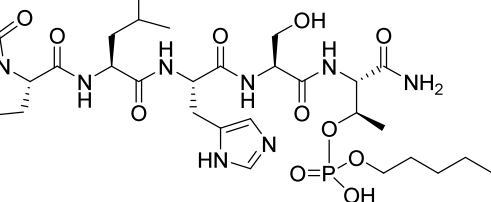
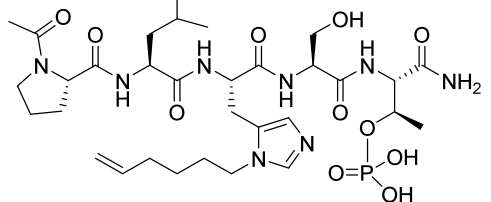
**Solid-phase peptide synthesis.** Fmoc-Thr(PO(OBzl)OH)-OH and other Fmoc protected amino acids were purchased from Novabiochem. Peptides were synthesized on NovaSyn®TGR resin (Novabiochem, cat. no. 01-64-0060) using standard Fmoc solid-phase protocols in N-Methyl-2-pyrrolidone (NMP). 1-O-Benzotriazole-N,N,N',N'-tetramethyluronium-hexafluoro-phosphate (HBTU) (5.0 eq.), hydroxybenzotriazole (HOBT) (5.0 eq.) and N,N-diisopropylethylamine (DIPEA) (10.0 eq.) were used as coupling reagents. Amino terminal acetylation was achieved using 1-acetylimidazole. Finished resins were washed with N,N-dimethylformamide (DMF), methanol, dichloromethane and diethyl ether and then dried under vacuum (overnight). For the synthesis of Pmab-containing peptides, (2*S*,3*R*)-4-[di-(tert-butyl)-oxyphosphinyl]-*N*-Fmoc-L-valine<sup>1</sup> was used in place Fmoc-Thr(PO(OBzl)OH)-OH.

**Derivatization on solid-phase using Mitsunobu reaction conditions.** Crude peptide resins prepared as outlined above (200 mg, 0.04 mmol) were swelled in dichloromethane (15 minutes) and then treated with triphenylphosphine (262 mg, 1.0 mmol), diethyl azidodicarboxylate (DEAD) (0.46 mL, 40% solution in toluene, 1.0 mmol) and alcohols R = **a – i**, Supplementary **Fig. 1**) (1.0 mmol) in dry dichloromethane at room temperature (2 h), then washed (dichloromethane), dried under vacuum (2 h) and cleaved by treatment with trifluoroacetic acid as indicated below.

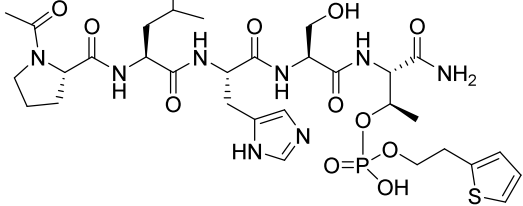
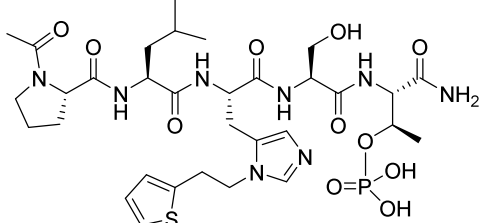
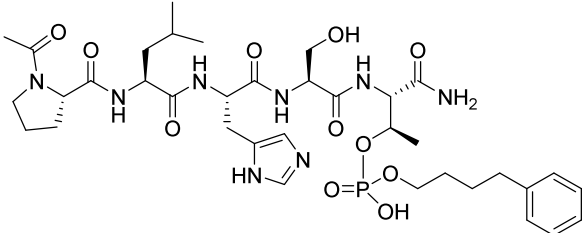
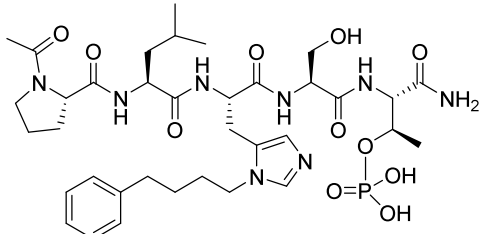
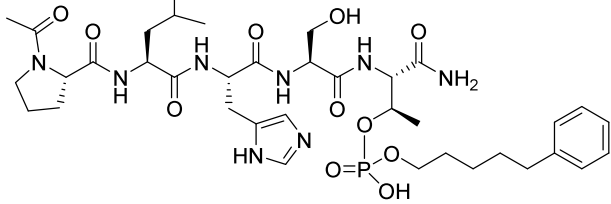
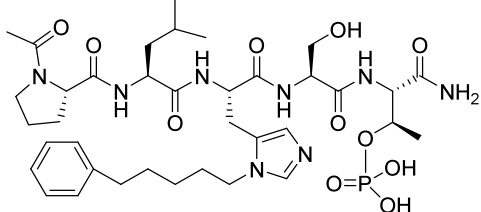
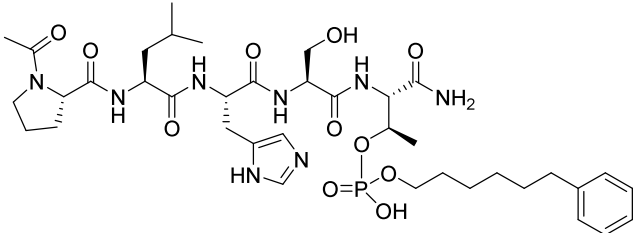
**Peptide cleavage and purification.** Peptide resins as prepared above (200 mg) were cleaved by treatment with trifluoroacetic acid : triisopropylsilane : H<sub>2</sub>O (90 : 5 : 5) (5 mL, 4 h). The resin was removed by filtrations and the filtrate was concentrated under vacuum, then peptide was precipitated by the addition of diethyl ether and the precipitate washed with ether. The resulting solid was dissolved in 50% aqueous acetonitrile (5 mL) and purified by reverse phase preparative HPLC using a Phenomenex C<sub>18</sub> column (21 mm dia x 250 mm, cat. no: 00G-4436-P0) with a linear gradient from 0% aqueous acetonitrile (0.1% trifluoroacetic acid) to 100% acetonitrile (0.1% trifluoroacetic acid) over 30 minutes at a flow rate of 10.0 mL/minute. Lyophilization gave the products as white powders (Supplementary **Tables 1, 2 and 6**).

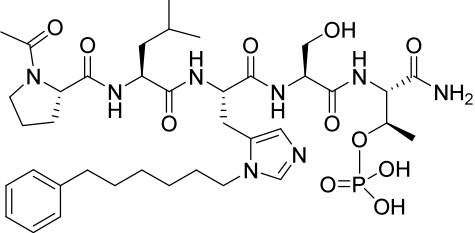
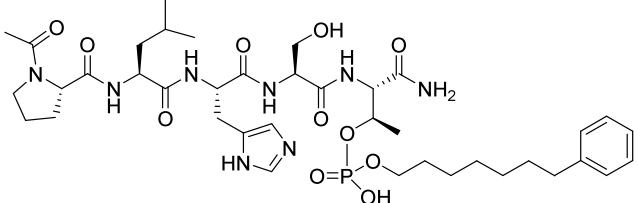
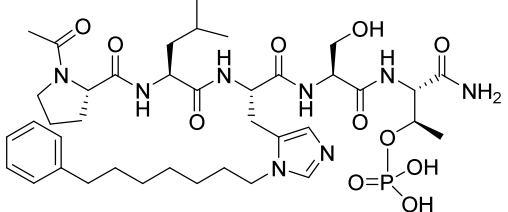
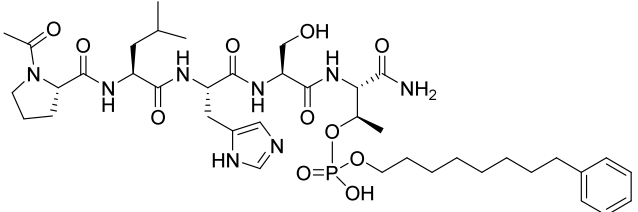
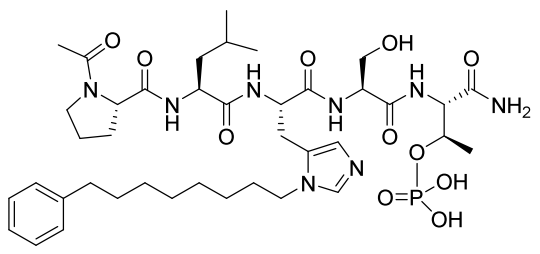
**Supplementary Table 1. Electrospray ionization (ESI) mass spectral data.**

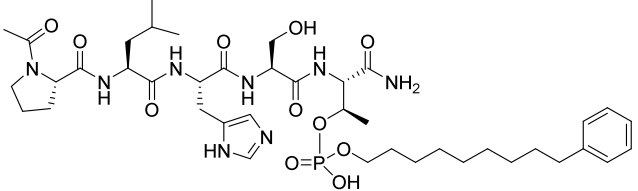
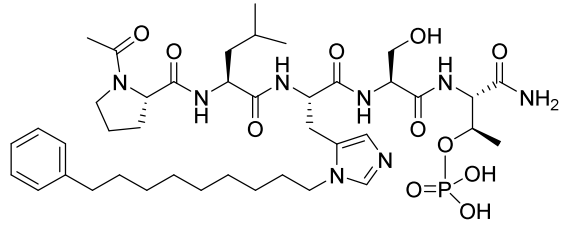
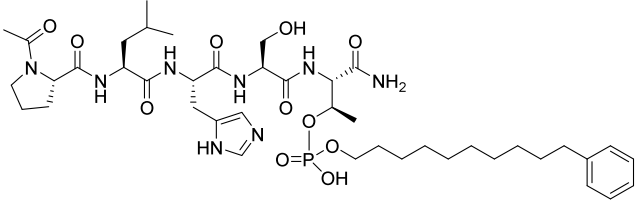
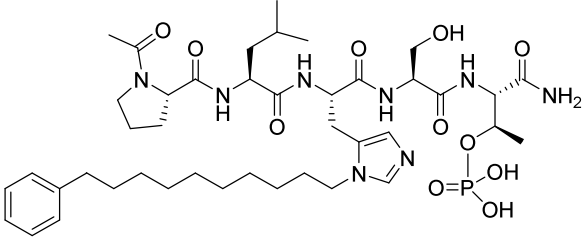
No.	Peptide Structure	Expected (M + H) <sup>+</sup>	Observed (M + H) <sup>+</sup>
3a		689.3	689.3
4a		689.3	689.3

<p><b>3b/4b<sup>†</sup></b></p>	 <p><b>3b</b></p> <p><b>4b</b></p>	<p>763.3</p>	<p>763.3</p>
<p><b>3c</b></p>		<p>747.3</p>	<p>747.3</p>
<p><b>4c</b></p>		<p>747.3</p>	<p>747.3</p>
<p><b>3d</b></p>		<p>757.4</p>	<p>757.4</p>
<p><b>4d</b></p>		<p>757.4</p>	<p>757.3</p>



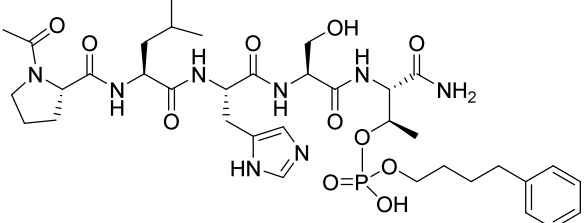
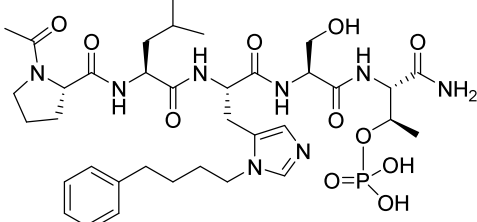
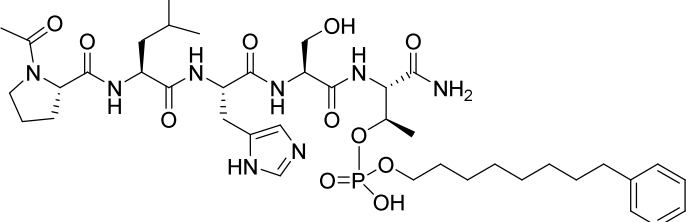
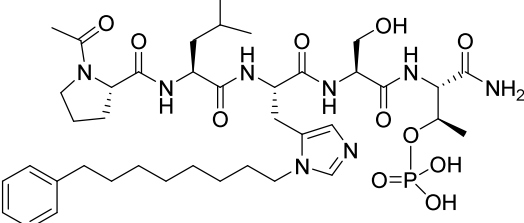
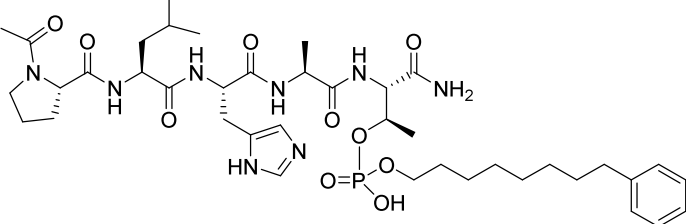
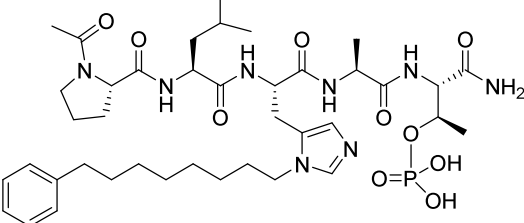
3e		785.2	785.2
4e		785.2	785.2
3f		807.4	807.3
4f		807.4	807.4
3g		821.4	821.2
4g		821.4	821.2
3h		835.4	835.2

4h		835.4	835.2
3i		849.4	849.3
4i		849.4	849.3
3j		863.4	863.5
4j		863.4	863.5

3k		877.5	877.3
4k		877.5	877.3
3l		891.5	891.3
4l		891.5	891.3

†These two products are not separable on preparative HPLC.

Supplementary Table 2. HRMS of selected peptides.

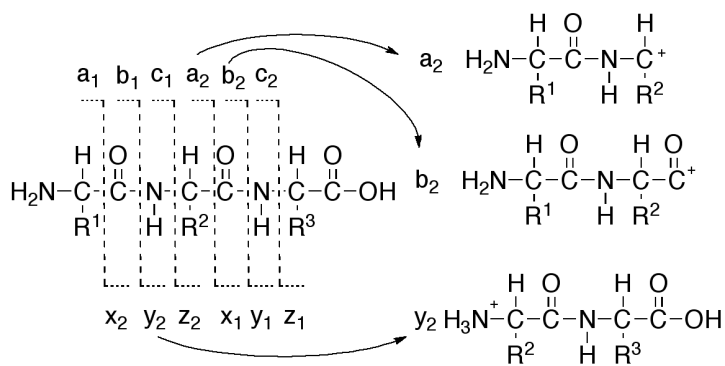
No.	Peptide Structure	Expected (M + H) <sup>+</sup>	Observed (M + H) <sup>+</sup>
3f		807.3801	807.3812
4f		807.3801	807.3797
3j		863.4427	863.4439
4j		863.4427	863.4446
3j (S4A)		847.4478	847.4463
4j (S4A)		847.4478	847.4466

**ELISA-based PBD-binding inhibition assay.** A biotinylated p-T78 peptide was first diluted with 1X coating solution (KPL Inc., Gaithersburg, MD) to the final concentration of 0.3  $\mu$ M, and then 100  $\mu$ l of the resulting solution was immobilized onto a 96-well streptavidin-coated plate (Nalgen Nunc, Rochester, NY). The wells were washed once with PBS plus 0.05% Tween20 (PBST), and incubated with 200  $\mu$ L of PBS plus 1% BSA (blocking buffer) for 1 h to prevent non-specific binding. Mitotic 293A lysates expressing HA-EGFP-Plk1 were prepared in TBSN buffer ( $\sim$  60  $\mu$ g total lysates in 100  $\mu$ L buffer), mixed with the indicated amount of the competitors (p-T78 peptide and its derivative compounds), provided immediately onto the biotinylated peptide-coated ELISA wells, and then incubated with constant rocking for 1 h at 25  $^{\circ}$ C. Following the incubation, ELISA plates were washed 4 times with PBST. To detect bound HA-EGFP-Plk1, the plates were probed for 2 h with 100  $\mu$ L/well of anti-HA antibody at a concentration of 0.5  $\mu$ g/mL in blocking buffer and then washed 5 times. The plates were further probed for 1 h with 100  $\mu$ L/well of HRP-conjugated secondary antibody (GE Healthcare, Piscataway, NJ) at a 1:1,000 dilution in blocking buffer. The plates were washed 5 times with PBST and incubated with 100  $\mu$ L/well of 3,3',5,5'-tetramethylbenzidine (TMB) solution (Sigma, St. Louis, MO) as a substrate until a desired absorbance was reached. The reactions were stopped by the addition of 100  $\mu$ L/well of stop solution (Cell Signaling Technology, Danvers, MA). The optical density (O.D.) was measured at 450 nm by using an ELISA plate reader (Molecular Devices, Sunnyvale, CA). Data are shown in **Table 1** of the published text and Supplementary **Fig. 5** and **6**.

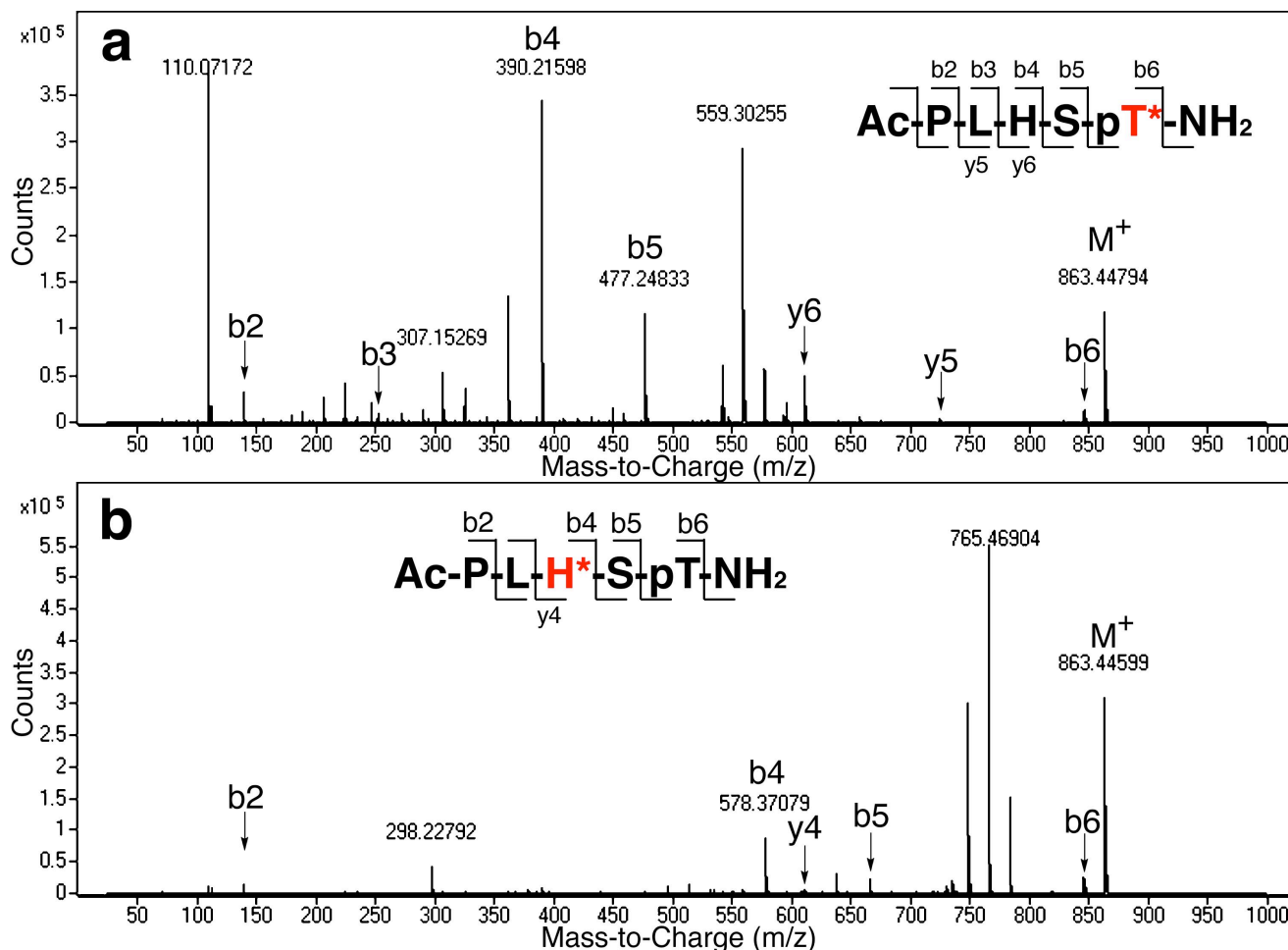
**MS-MS Analysis of peptides 3j and 4j.** Tandem MS studies were undertaken to clarify the site of  $C_6H_5C_8H_8$ -adduct addition in peptides **3j** and **4j**. Mass spectrometry data were acquired on an Agilent 6520 Accurate-Mass Q-TOF LC/MS System, (Agilent Technologies, Inc., Santa Clara, CA) equipped with a dual electro-spray source, operated in the positive-ion mode. Separation was performed on Zorbax 300SB-C18 Poroshell column (2.1 mm x 75 mm; particle size 5  $\mu$ m). The analytes were eluted with solvent system 0.1% formic acid in  $H_2O$ / 0.1% formic acid in acetonitrile at a flow rate of 1 ml/min with a 5 to 100% organic gradient over 4 minutes and holding organic for 1 minute. The instrument was used in either full-scan TOF mode or product ion scan (MS/MS) mode. MS source parameters were set with a capillary voltage of 4 kV, the fragmentor voltage of 175 V and skimmer 65 V. The gas temperature was 350  $^{\circ}$ C, drying gas flow 12 L/min and nebulizer pressure 55 psig. High purity nitrogen was used as a collision gas. Data were acquired at high resolution (1,700  $m/z$ ), 4 GHz. TOF-MS mass spectra were recorded across the range 100–1600  $m/z$ . Q-TOF-MS/MS experiments were carried out in the range 50–1000  $m/z$  with a scan rate of 1.4 spectra/s with collision energy of 35 V. Data acquisition and analysis were performed using MassHunter Workstation Software (version B.02.00). To maintain mass accuracy, an internal mass calibration solution, containing reference ions  $m/z$  121.050873 and  $m/z$  922.009798, was infused continuously during the LC/MS runs.

Fragmentation of peptides typically occurs sequentially along the peptide backbone at the sites of the carboxamide groups. For each residue starting from the N-terminal end of the peptide, fragments are given sequential alphabetical designations starting with “a”; for example, a1, b1, c1 for residue 1; a2, b2, c2 for residue 2, etc as shown in the Supplementary **Fig. 2** (below). In similar fashion starting from the C-terminal end of the peptide, fragments for each residue are designated alphabetically starting from “z” as shown in the Figure. The most commonly observed ions are of the “a”, “b” and “y” type. For peptide **3j** the MS –fragments

were consistent with the  $C_6H_5C_8H_8$ -adduct being on the pThr residue, with key fragments being  $b_6+H$  and  $b_5$  (see the Supplementary **Fig 3a** and Supplementary **Table 3**). For peptide **4j**, fragmentation was consistent with the  $C_6H_5C_8H_{16}$ -adduct being on the His residue, with key fragments being  $b_4$  and  $y_4$  (see Supplementary **Fig. 3b** and Supplementary **Table 4**). It should be noted that the data did not indicate the site of adduct attachment on the His residue.



**Supplementary Figure 2.** Demonstration of fragmentation nomenclature.



**Supplementary Figure 3.** MS-MS spectrum of peptides. (a) Peptide **3j**. (b) Peptide **4j**.







$b_6 + H - H_3PO_4$		$C_{40}H_{59}N_7O_7^{+}$	749.44705	749.4485
$b_5$		$C_{36}H_{53}N_6O_6^+$	665.40211	665.4032
$a_5$		$C_{35}H_{53}N_6O_5^+$	637.40720	637.4081
$y_4$		$C_{27}H_{44}N_6O_8P^+$	611.29528	611.2970
$b_4$		$C_{33}H_{48}N_5O_4^+$	578.37008	578.3708
$y_4 - H_3PO_4$		$C_{27}H_{41}N_6O_4^+$	513.31838	513.3198
$a_4 - b_3$		$C_{19}H_{28}N_3^+$	298.22777	298.2279

b <sub>2</sub>		C <sub>7</sub> H <sub>10</sub> NO <sub>2</sub> <sup>+</sup>	140.07060	140.0700
----------------	---	---	-----------	----------

## X-ray Crystallography

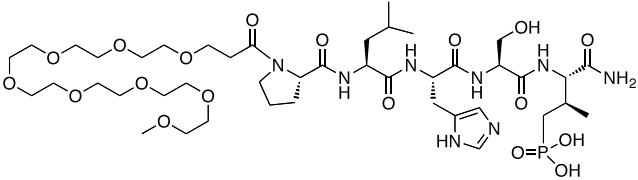
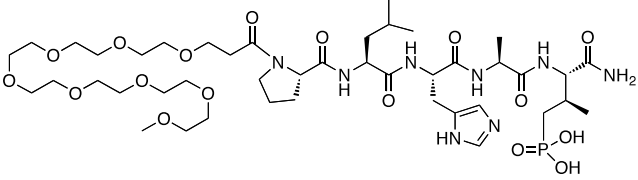
**Protein purification and crystallization.** Plk1 PBD protein (residues 371-603) was purified as previously described.<sup>2</sup> Crystals were grown using the hanging drop vapor diffusion method. PBD protein at 12 mg/mL in 10 mM Tris pH 8, 0.5 M NaCl, 10 mM DTT, 2% DMSO and 2 mM compound **4j** was mixed with an equal volume of reservoir solution consisting of 15% (w/v) PEG 3350, 0.1 M glycine pH 9 and 300 mM NaCl. Crystals appeared overnight and reached maximum size over several days.

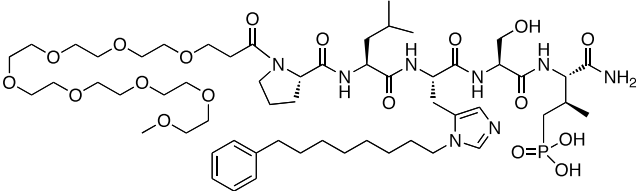
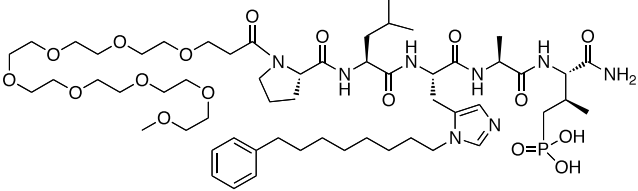
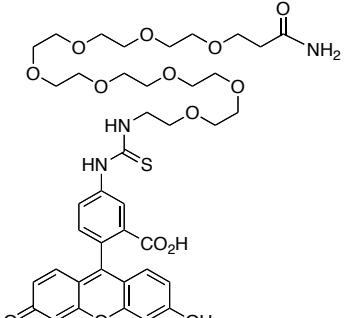
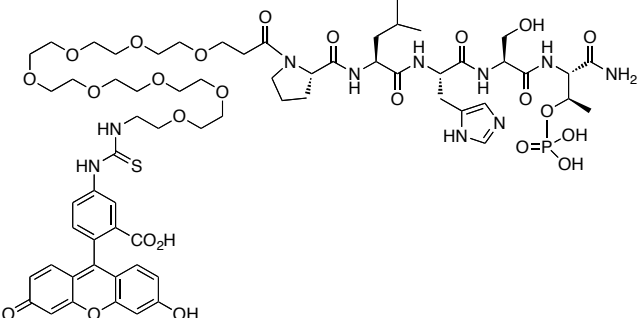
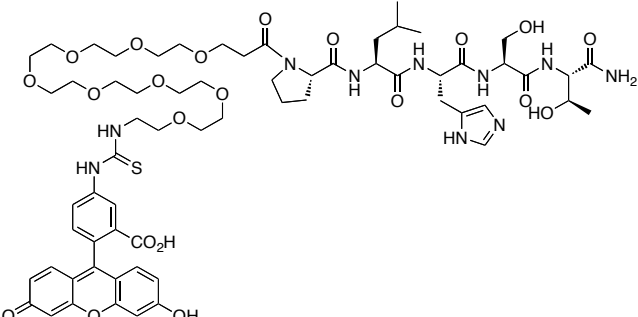
**Data collection, and structure determination and refinement.** Crystals were cryo-protected in 33.3% (w/v) PEG3350, 500 mM NaCl, 0.1 M glycine pH 9, 2 mM **4j**, 2 % DMSO and 10 mM DTT, and data were collected at 100 K on a Mar345 image plate detector with a Rigaku RU-300 home X-ray source. The data were processed with the HKL<sup>3</sup> and CCP4<sup>4</sup> software suites. The structure was solved by molecular replacement using AMoRe<sup>5</sup> using chain A of structure 3FVH<sup>2</sup> (RCSB accession code) as a search model, and refined using PHENIX<sup>6</sup> with manual fitting in XtalView.<sup>7</sup> The final model contains 90.6%, 8.4%, 0.5% and 0.5% (Leu 490) of the protein residues in the most favorable, allowed, generously allowed, and disallowed regions of Ramachandran plot, respectively. The strained conformation of Leu 490 appears to be stabilized by ligand binding. The figure was created using Molscript<sup>8</sup> and PyMOL (<http://www.pymol.org/>).

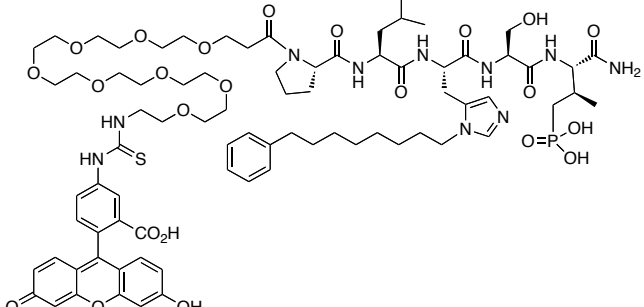
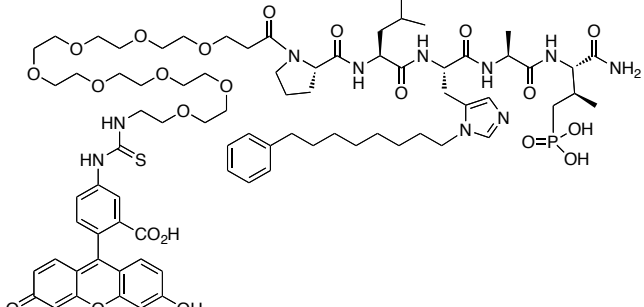
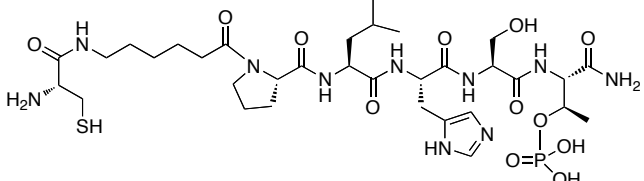
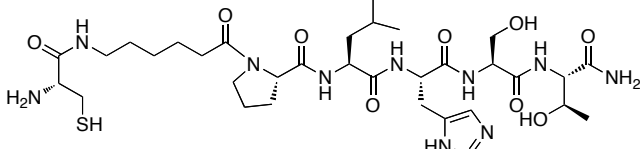
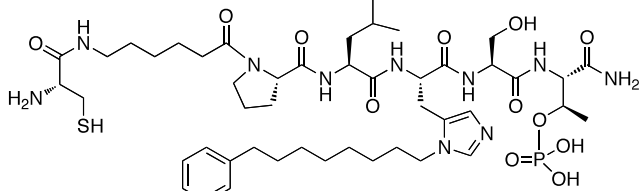
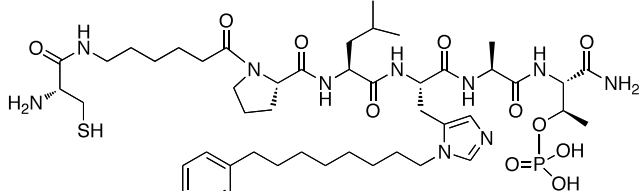
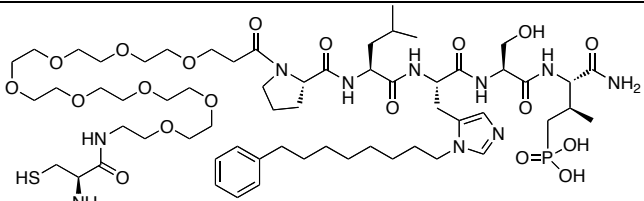
**Solid-phase synthesis of PEGylated peptides.** PEGylated peptides were synthesized on NovaSyn<sup>®</sup>TGR resin (0.1 mmol resin was used for each peptide, Novabiochem, cat. no. 01-64-0060, loading 0.20-0.30 mmol/g) using standard Fmoc solid-phase protocols in a polypropylene column with a filter (Thermo Scientific. Cat. no. 29924, volume: 10 mL). For each coupling cycle, Fmoc protected amino acid (5.0 eq.), 1-O-benzotriazole-N, N, N', N'-tetramethyl-uronium-hexafluoro-phosphate (HBTU) (5.0 eq.), hydroxybenzotriazole (HOBT) (5.0 eq.) and N, N-diisopropylethylamine (DIPEA) (10 eq.) were used. Coupling proceeded for 2 hours at room temperature in N-Methyl-2-pyrrolidone (NMP, 4.0 mL), followed by DMF washing (3.0 mL x 5). The resin was treated with 20% piperidine in N, N'-dimethylformamide (4.0 mL) for 20 minutes at room temperature and washed (DMF, 3.0 mL x 5) before the next coupling. The amino-terminus was acylated with m-dPEG<sup>®</sup>8-acid (or Fmoc-N-amido-dPEG<sup>®</sup>8-NHS ester) by reacting with HBTU (5.0 eq.), HOBT (5.0 eq.) and DIPEA (10.0 eq.) for 4h at room temperature. Peptides were tagged with FITC by reacting with 5 equivalents of fluorescein isothiocyanate in the presence of 5 equivalents of N, N-diisopropylethylamine in N, N-dimethylformamide (overnight). The resin was washed with DMF (4.0 mL x 5), methanol (4.0 mL x 5), methylene chloride (4.0 mL x 5) and diethyl ether (4.0 mL x 5), then dried under vacuum (overnight).

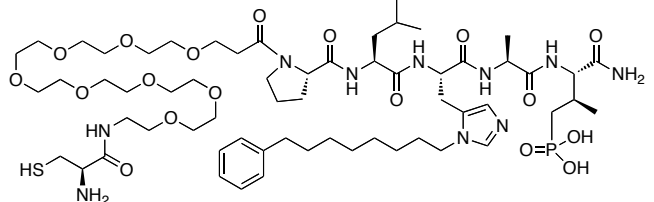
**Resin cleavage and HPLC purification of PEGylated peptide products.** Peptides were cleaved from the resin (~ 200 mg) by treatment with trifluoroacetic acid: triisopropylsilane: H<sub>2</sub>O (4.0 mL, 0.1 mL, 0.1 mL) for 4 hours at room temperature. The resin was removed by filtration and the filtrate was concentrated under vacuum, then precipitated with diethyl ether (5.0 mL), and the precipitate was washed with diethyl ether (5 mL x 3). The resulting solid was dissolved in 50% aqueous acetonitrile (5 mL) and purified by reverse phase preparative HPLC using a Phenomenex C<sub>18</sub> column (21 mm dia x 250 mm, cat. no: 00G-4436-P0). Lyophilization gave products as white powders (Supplementary **Tables 5** and **6** and **Fig. 4**).

**Supplementary Table 5. Electrospray ionization (ESI) mass spectral data.<sup>a</sup>**

No.	Peptide Structure	Expected (M + H) <sup>+</sup>	Observed (M + H) <sup>+</sup>
5		1025.5	1025.2
5(S4A)		1009.5	1009.2

6		1213.7	1213.3
6(S4A)		1197.7	1197.4
7		830.3	830.3
8		1445.6	1445.4
8(pT5T)		1365.6	1365.4

9		1631.7	1631.5
9(S4A)		1615.7	1615.6
10		848.4	Previously Reported <sup>b</sup>
10(pT5T)		768.4	Previously Reported <sup>b</sup>
11		1037.5	1037.5
11(S4A)		1021.5	1021.3
12		1345.7	1345.5

<b>12(S4A)</b>		1329.7	1329.6
----------------	---	--------	--------

<sup>a</sup>All FITC-labeled peptides were  $\geq 99\%$  pure by HPLC analysis. <sup>b</sup>Previously reported in reference 2.

**Supplementary Table 6. Purity of non-FITC-labeled peptides.<sup>a</sup>**

Peptide Number	Purity	HPLC Method	Peptide Number	Purity	HPLC Method
<b>3a</b>	97%	A	<b>4a</b>	97%	A
<b>3b/4b</b>	> 99%	A			
<b>3c</b>	> 99%	A	<b>4c</b>	> 99%	A
<b>3d</b>	> 99%	A	<b>4d</b>	> 99%	A
<b>3e</b>	94%	A	<b>4e</b>	> 99%	A
<b>3f</b>	99%	A	<b>4f</b>	99%	A
<b>3g</b>	> 99%	A	<b>4g</b>	90%	A
<b>3h</b>	> 99%	A	<b>4h</b>	93%	A
<b>3i</b>	> 99%	A	<b>4i</b>	92%	A
<b>3j</b>	99%	A	<b>4j</b>	> 99%	A
<b>3j(S4A)</b>	95%	A	<b>4j(S4A)</b>	> 99%	A
<b>3k</b>	> 99%	A	<b>4k</b>	90%	A
<b>3l</b>	98%	A	<b>4l</b>	98%	A
<b>5</b>	> 99%	B	<b>6</b>	> 99%	B
<b>5(S4A)</b>	> 99%	B	<b>6(S4A)</b>	96%	B
<b>11</b>	97%	A	<b>12</b>	> 99%	B
<b>11(S4A)</b>	> 99%	B	<b>12(S4A)</b>	89%	B

<sup>a</sup>Determined by reverse phase HPLC using the indicated conditions:

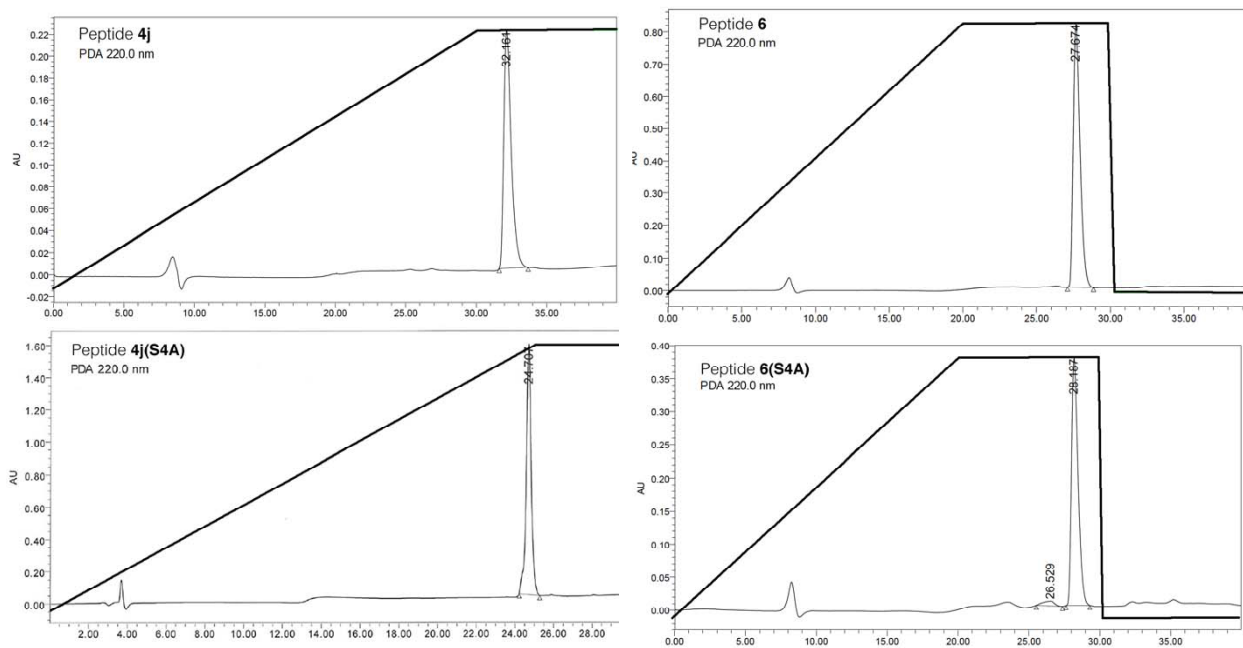
### Method A

Detection = 220 nm; Solvent A = H<sub>2</sub>O, 0.1% TFA; Solvent B = MeCN, 0.1%TFA

T (min)	0	30	40	40.1
B%	0	100	100	100
Flow (mL/min)	1	1	1	0

### Method B

T (min)	0	20	30	30.1	40	40.1
B%	0	100	100	0	0	0
Flow (mL/min)	1	1	1	1	1	0



**Supplementary Figure 4.** Analytical HPLCs of select peptides. Conditions as indicated in Supplementary Table 6.

### **PBD Fluorescence polarization competition binding assays for Plk1.**

Competition assays for the Plk1 PBD were also performed essentially as described.<sup>9-12</sup> In brief, 5-carboxyfluorescein-GPMQSpTPLNG-OH (**14**) (final concentration: 2 nM) was incubated with the Plk1 PBD (final concentration: 10 nM) in the presence of the test peptides (final concentrations of buffer components: 50 mM NaCl, 10 mM Tris (pH 8.0), 1 mM EDTA, 0.1% Nonidet P-40 substitute, 1 mM dithiothreitol, and 2% DMSO.) Fluorescence polarization was analyzed after 30 min. Inhibition curves were fitted using SigmaPlot (SPSS). All experiments were performed in triplicate. Numerical IC<sub>50</sub> values are shown in Supplementary **Table 8** and data plots are shown in Supplementary **Fig. 9**.

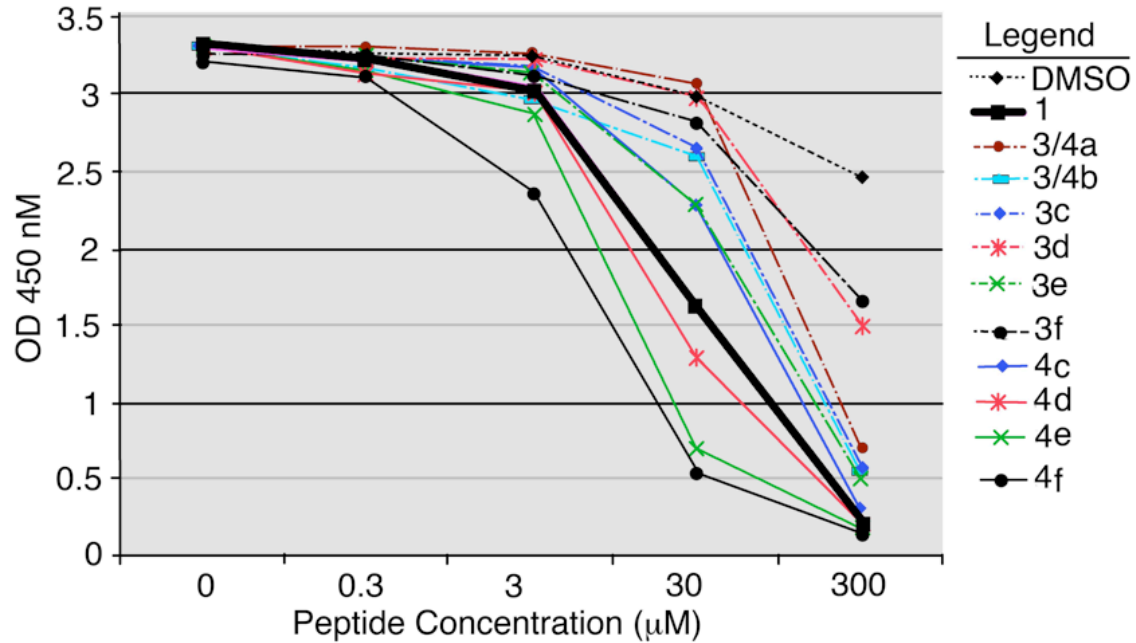
**PBD Fluorescence polarization binding assays for Plk1, Plk2 and Plk3.** Binding assays for the PBDs of Plk1, Plk2, and Plk3 were performed essentially as described.<sup>9-12</sup> In brief, fluorescein-labeled peptides (final concentration: 2 nM) were incubated with the PBDs of Plk1, Plk2, and Plk3, respectively (final concentrations of buffer components: 50 mM NaCl, 10 mM Tris (pH 8.0), 1 mM EDTA, 0.1% Nonidet P-40 substitute, and 1 mM dithiothreitol). Proteins were used at final concentrations ranging from 0.039 nM to 2560 nM. Fluorescence polarization was analyzed 30 min after mixing of all components in the 384-well format using a Tecan Infinite F500 plate reader. Binding curves were fitted using SigmaPlot (SPSS). All experiments were performed in triplicate. K<sub>d</sub>-values were extrapolated from the binding curves as the concentration at which 50% of the fluorescein-labeled peptides are protein-bound. For the high-affinity ligand **9**, this method may lead to an overestimation of the K<sub>d</sub> due to receptor depletion. Precise experimental determination of the K<sub>d</sub> of **9** would require its use at concentrations < 2 nM; however, the use of **9** at concentrations < 2 nM was accompanied by an insufficient signal to noise ratio. Dissociation constants (K<sub>d</sub>) are shown in Supplementary **Table 9** and data plots are shown in Supplementary **Fig. 10**.

**Peptide pull-down assay.** Peptide pull-down assays were carried out essentially as described previously.<sup>2</sup> To study Plk1 PBD-binding specificity, p-T78 peptide or its derivatives were covalently conjugated to beads using SulfoLink Coupling Gel (Pierce, Rockford, IL) via either an N-terminal Cys-(CH<sub>2</sub>)<sub>6</sub>-CO linker [peptide **10** for **1**; peptide **10(pT5T)** for **1(pT5T)**; peptide **11** for **4j** and peptide **11(S4A)** for **4j(S4A)**] or an N-terminal Cys residue conjugated to PEG moiety [peptide **12** for **6** and peptide **12(S4A)** for **6(S4A)**]. Mitotic lysates expressing Plk1-3 were prepared from 293T cells transfected with Flag-Plk1 (K82M), Flag-Plk2 (K108M) or Flg-Plk3 (K52R) (a gift of Wei Dai, New York University School of Medicine, NY) and treated with 200 ng/ml of nocodazole for 16 h. After incubating the cell lysates prepared in TBSN buffer {20 mM Tris-Cl (pH8.0), 150 mM NaCl, 0.5% Np-40, 5 mM EGTA, 1.5 mM EDTA, 20 mM *p*-nitrophenylphosphate and protease inhibitor cocktail (Roche, Nutley, NJ)} with the bead-immobilized ligands for 2 h at 4 °C, the ligand-associating proteins were precipitated, washed, boiled in sodium dodecyl sulfate (SDS) sample buffer, separated by 8% SDS-polyacrylamide gel electrophoresis (PAGE), and then subjected to immunoblotting analysis with anti-Flag antibody and the enhanced chemiluminescence (ECL) detection system (Pierce). The same membrane was also stained with Coomassies (CBB). Signal intensities were quantified using Image J program. Results are shown in **Fig. 2a** of the published text.

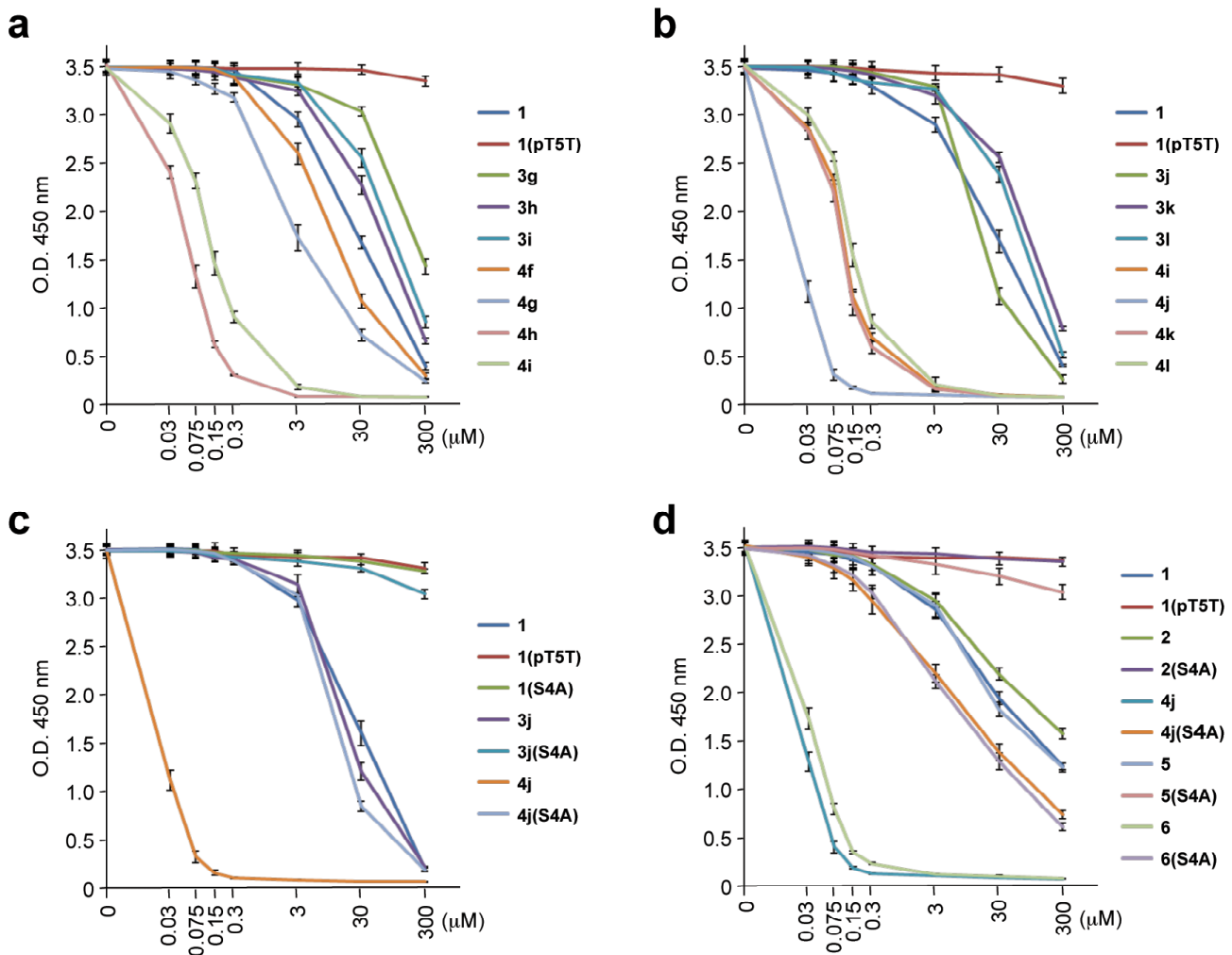


**Cell culture, analysis of cellular proliferation, aberrant mitotic population and indirect immunofluorescence microscopy.** HeLa cervical carcinoma cell line CCL2, 293A and 293T cells were cultured as recommended by the American Type Culture Collection (Manassas, VA). To prepare mitotic 293A cells expressing HA-EGFP-Plk1, cells were infected with adenovirus expressing HA-EGFP-Plk1 and arrested with 200 ng/mL of nocodazole for 16 h. To analyze the effect of the indicated compounds in cultured cells, logarithmically growing HeLa cells were treated with 200  $\mu$ M of the indicated compounds for 24 h (a sufficient amount of time to enrich mitotically-arrested cells). BI 2536 was purchased from Selleck Chemicals LLC (Boston, MA) (purity > 99%) and was used at 100 nM for the indicated lengths of time. The resulting cells were then treated with Hoechst 33342 for 10 min, fixed with 4% paraformaldehyde and then subjected to immunostaining analyses. In a separate experiment, HeLa cells were arrested with 2.5 mM thymidine for 16 h and released into fresh medium. Four hours after release, cells were treated with 200  $\mu$ M of the compounds, harvested at the indicated time points, and then analyzed. Indirect immunofluorescence studies were performed as described previously,<sup>13</sup> using anti-Plk1 (Santa Cruz Biotechnologies, Santa Cruz, CA) and anti- $\alpha$ -tubulin (Sigma) antibodies followed by Texas red (red) and Alexa Fluor 488 (green)-conjugated secondary antibodies, respectively. Confocal images were acquired using a Zeiss LSM510 system mounted on a Zeiss Axiovert 100 M microscope (Carl Zeiss MicroImaging, Inc., Thornwood, NY). Results are shown in **Fig. 2 (b-e)** of the published text.

## SUPPLEMENTARY RESULTS



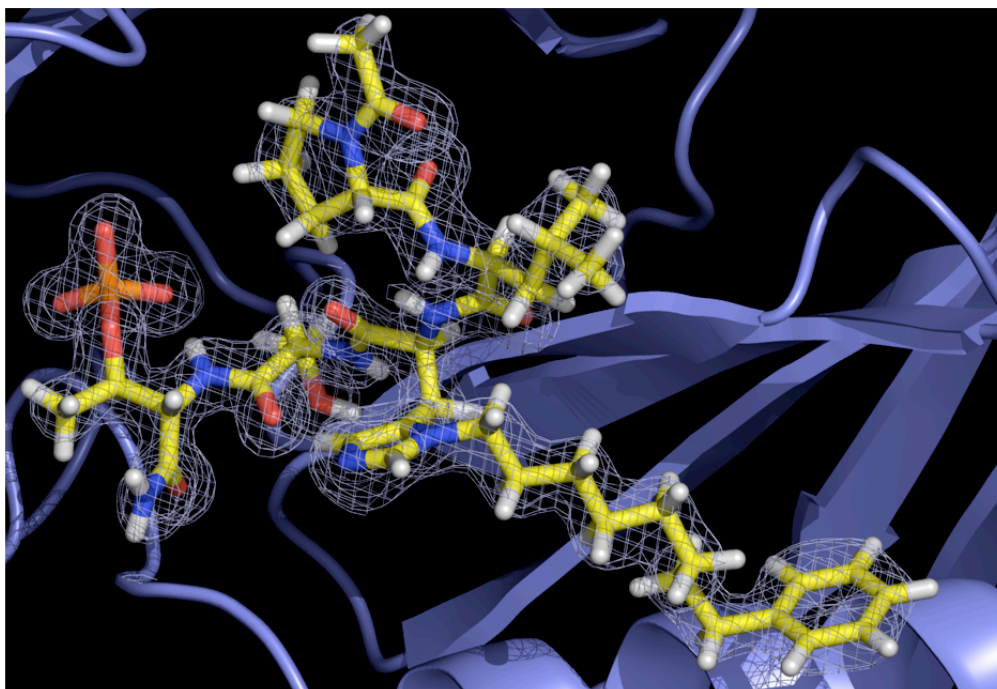
**Supplementary Figure 5.** Inhibition of Plk1 PBD by various PLHSpT-derived compounds. ELISA-based PBD inhibition assays were performed essentially as described in the Methods using HA-EGFP-Plk1-expressing mitotic 293A cell lysates. Optical densities (O.D.) for each sample were measured at 450 nm by using an ELISA plate reader.



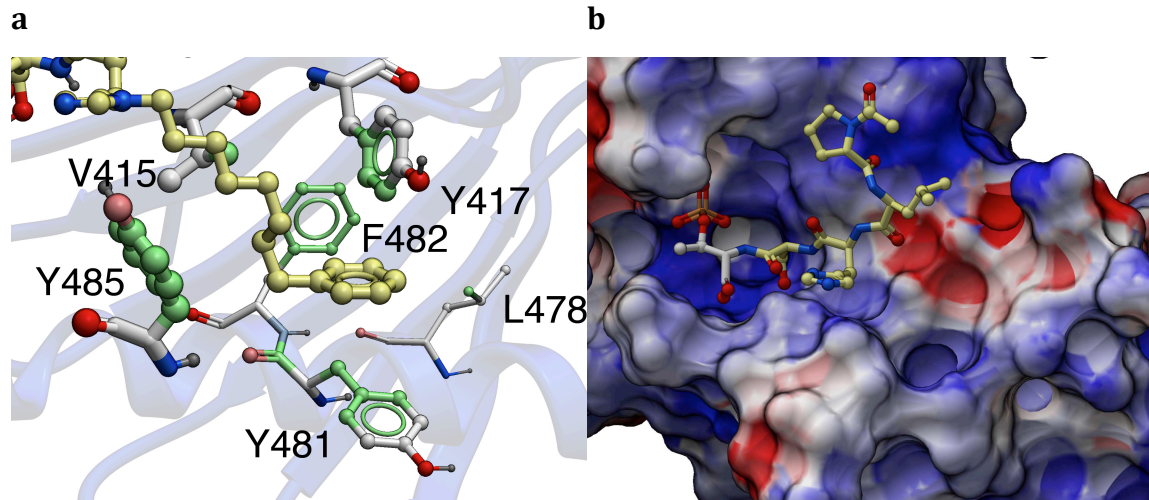
**Supplementary Figure 6.** Inhibition of Plk1 PBD by various PLHSpT-derived compounds. (a-d) ELISA-based PBD inhibition assays were performed essentially as described in the Methods using HA-EGFP-Plk1-expressing mitotic 293A cell lysates. Slight differences in the inhibition curves among the graphs are due to the differences in development time. Optical densities (O.D.) for each sample were measured at 450 nm by using an ELISA plate reader. Note that for reasons unknown, **4h** ( $n = 6$ ) inhibited PBD reproducibly better than **4i** ( $n = 7$ ). Multiple panels are employed to clarify data presentation. At least more than three independent experiments were carried out for each assay. Data represent mean values  $\pm$  s.d. (bars).

**Table 7. Data collection and refinement statistics (molecular replacement).**

	Crystal 1 name
<b>Data collection</b>	
Space group	P2 <sub>1</sub>
Cell dimensions	
<i>a</i> , <i>b</i> , <i>c</i> (Å)	35.3, 51.2, 58.0
$\alpha$ , $\beta$ , $\gamma$ (°)	90, 101.0, 90
Resolution (Å)	14.8-1.55 (1.61-1.55) *
<i>R</i> <sub>sym</sub> or <i>R</i> <sub>merge</sub>	0.048 (0.197)
<i>I</i> / $\sigma I$	31.7 (4.2)
Completeness (%)	99.8 (98.3)
Redundancy	6.2 (4.3)
<b>Refinement</b>	
Resolution (Å)	14.8 – 1.55
No. reflections	29160
<i>R</i> <sub>work</sub> / <i>R</i> <sub>free</sub>	0.1520 / 0.1896
No. atoms	
Protein	1768
Ligand/ion	60
Water	304
<i>B</i> -factors	
Protein	18.7
Ligand/ion	17.7
Water	31.7
R.m.s. deviations	
Bond lengths (Å)	0.012
Bond angles (°)	1.665



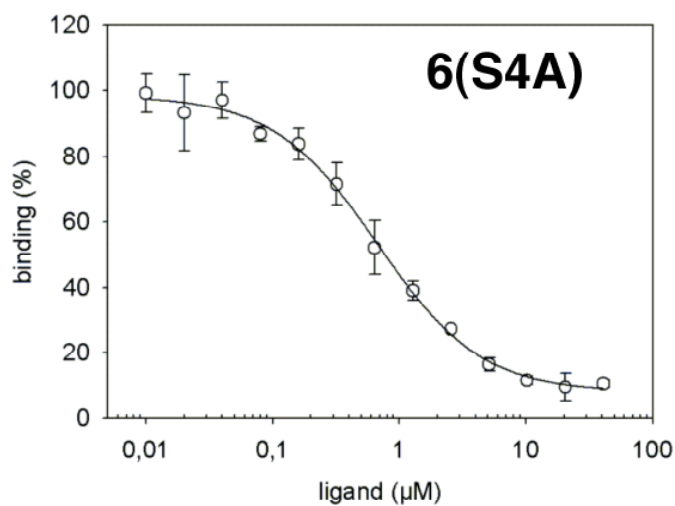
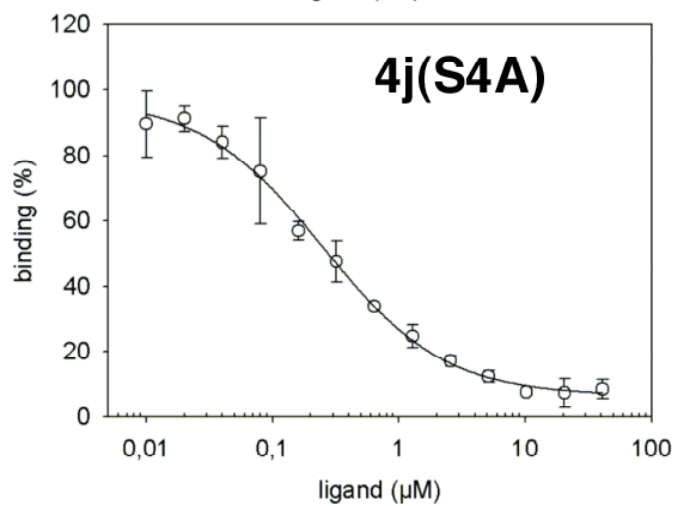
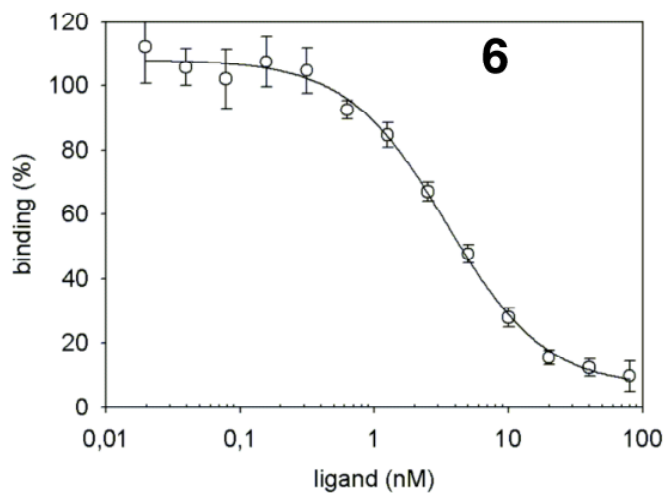
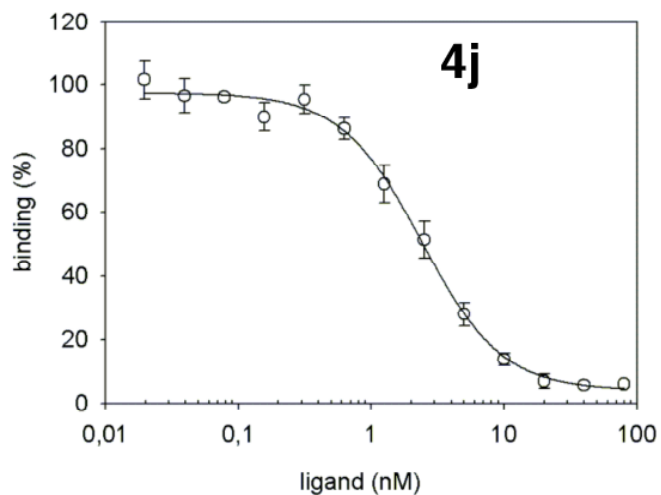
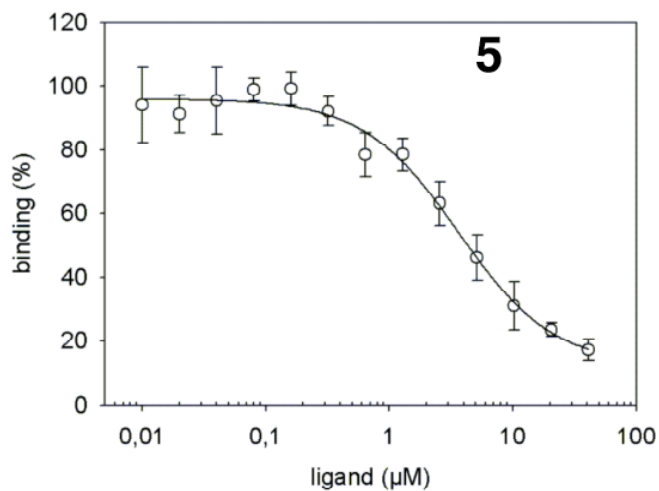
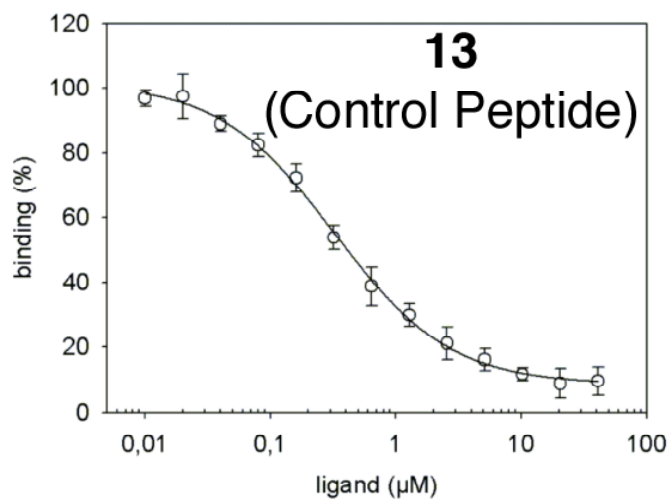
**Supplementary Figure 7.** SigmaA weighted 2Fo-Fc electron density map contoured at  $1\sigma$  and 1.55 Å resolution around peptide ligand **4j** (stick rendering). The PBD protein is shown in blue cartoon rendering.



**Supplementary Figure 8.** X-ray co-crystal structures of Plk1 PBD complexed with peptides **1** and **4j**. (a) The PBD•**4j** complex showing ball and stick rendering of key protein residues that interact with the His-(CH<sub>2</sub>)<sub>8</sub>-phenyl group (in yellow). Hydrophobic contact regions of protein residue side chains are shaded green, with the strength of interaction indicated by thickness. (b) Electrostatic surface PBD in complex with **1** with coloring based on an arbitrary electrostatic potential scale (positive = blue; negative = red). Peptide is rendered as ball and stick and colored by atom (blue = nitrogen; yellow = carbon; tan = phosphorus and red = oxygen). Graphics were generated using ICM Chemist Pro by Molsoft, Inc. ([www.molsoft.com](http://www.molsoft.com)).

**Supplementary Table 8: IC<sub>50</sub>-values of peptides competing with the binding of 5-carboxyfluorescein-GPMQSpTPLNG-OH (14) and the Plk1 PBD as determined by fluorescence polarization assays.**

<b>Peptide</b>	<b>Sequence</b>	<b>IC<sub>50</sub> [μM]</b>
<b>13</b>	H <sub>2</sub> N-MAGPMQSpTPLNGAKK-OH	0.41 ± 0.07
<b>4j</b>		0.0025 ± 0.0004
<b>4j(S4A)</b>		0.28 ± 0.06
<b>5</b>		4.46 ± 1.09
<b>6</b>		0.0044 ± 0.0002
<b>6(S4A)</b>		0.78 ± 0.12



**Supplementary Figure 9:** Results of fluorescence polarization assays showing inhibition of binding between 5-carboxyfluorescein-GPMQSpTPLNG-OH (**14**) and the Plk1 PBD by the indicated test.

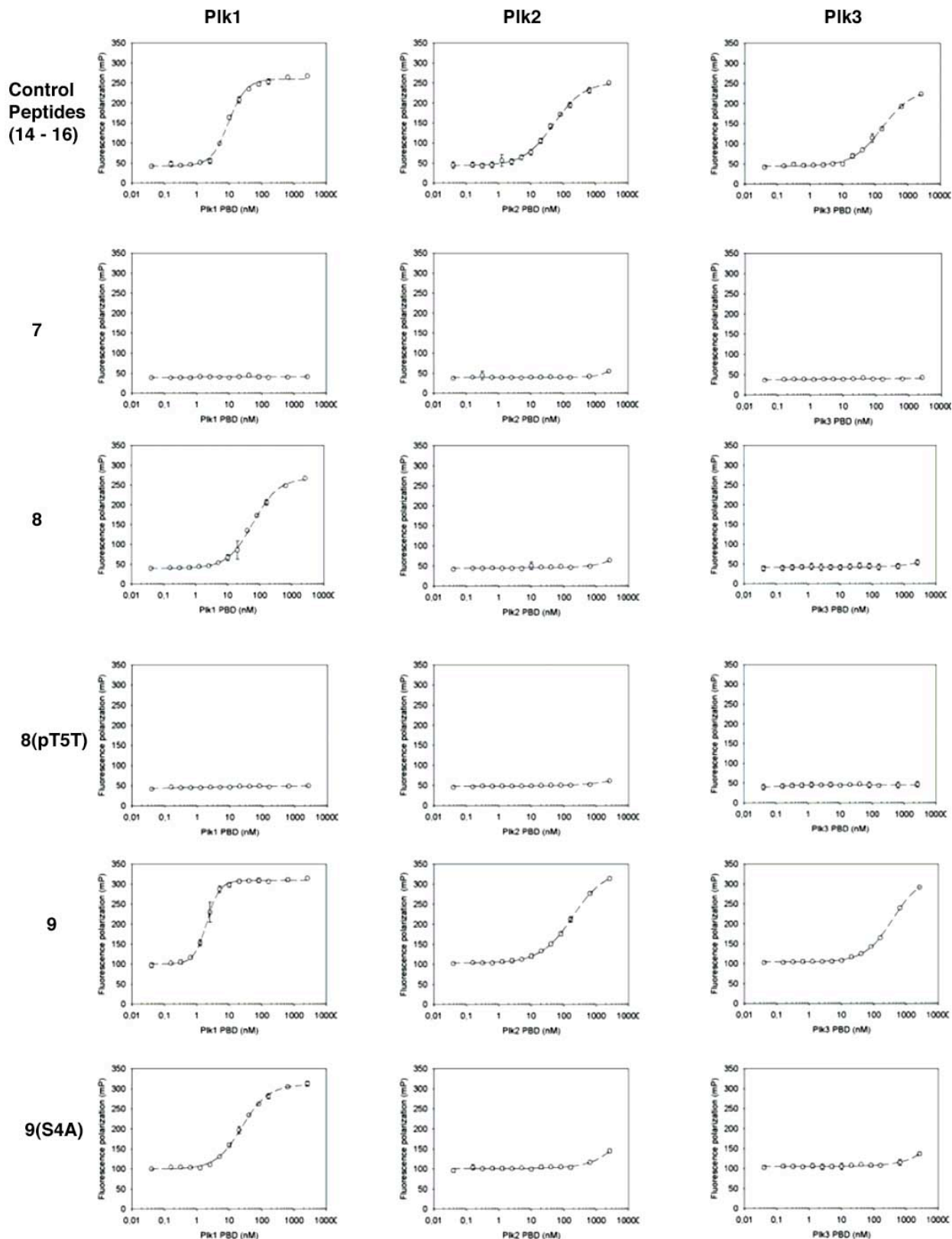
**Supplementary Table 9. Dissociation constants ( $K_d$ ) for binding between fluorescein-labeled peptides and the PBDs of Plk1, Plk2, and Plk3, respectively, as determined by fluorescence polarization assays.**

Peptide	Sequence	Plk1 PBD $K_d$ [nM]	Plk2 PBD $K_d$ [nM]	Plk3 PBD $K_d$ [nM]
<b>14</b>	5-Carboxyfluorescein-GPMQSpTPLNG-OH	$9.5 \pm 0.4$	n.a.	n.a.
<b>15</b>	5-Carboxyfluorescein-GPMQTSpTPKNG-OH	n.a.	$50.4 \pm 3.4$	n.a.
<b>16</b>	5-Carboxyfluorescein-GPLATSpTPKNG-OH	n.a.	n.a.	$167.2 \pm 17.3$
<b>8</b>		$59.8 \pm 4.8$	> 2560	> 2560
<b>8 (pT5T)</b>		> 2560	> 2560	> 2560
<b>9</b>		$2.0 \pm 0.2$ <sup>[a]</sup>	$194.2 \pm 39.8$	$460.1 \pm 99.2$
<b>9(S4A)</b>		$24.5 \pm 1.3$	> 2560	> 2560

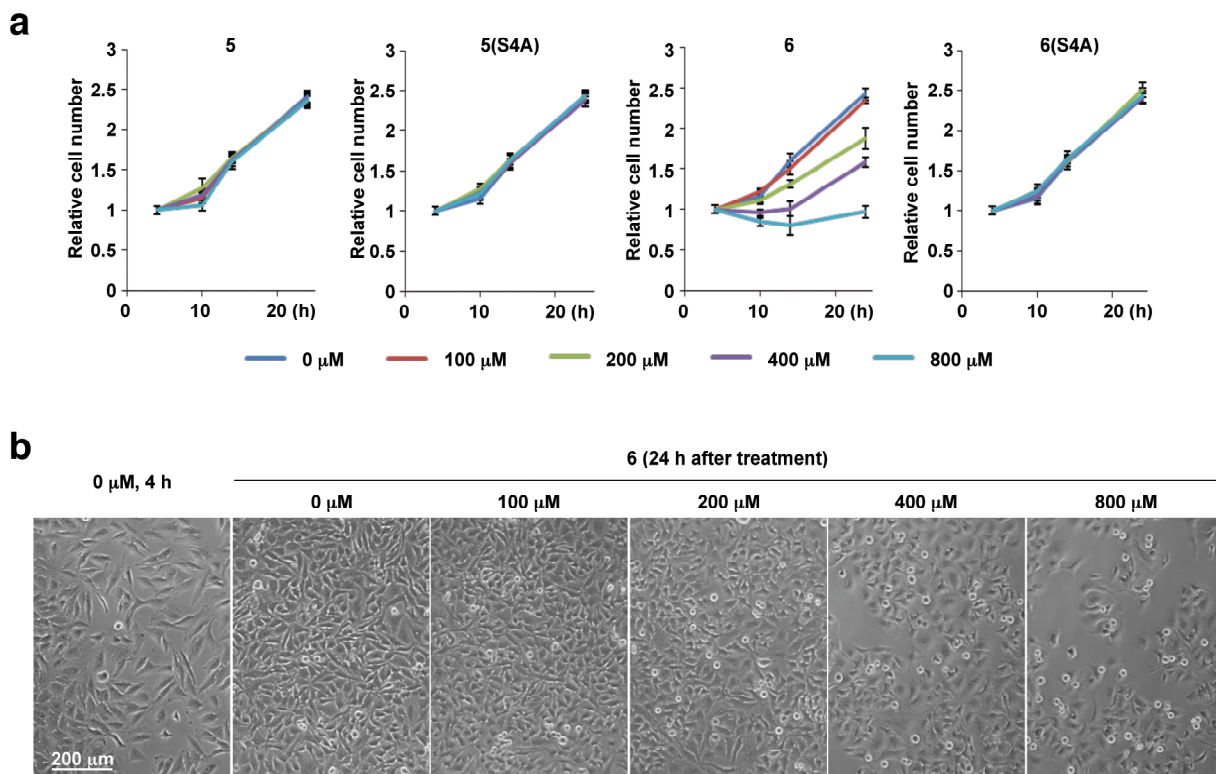
<sup>[a]</sup> Apparent  $K_d$  derived from the binding curve. The actual  $K_d$  of **9** is expected to be < 2 nM.

n.a.: not analyzed

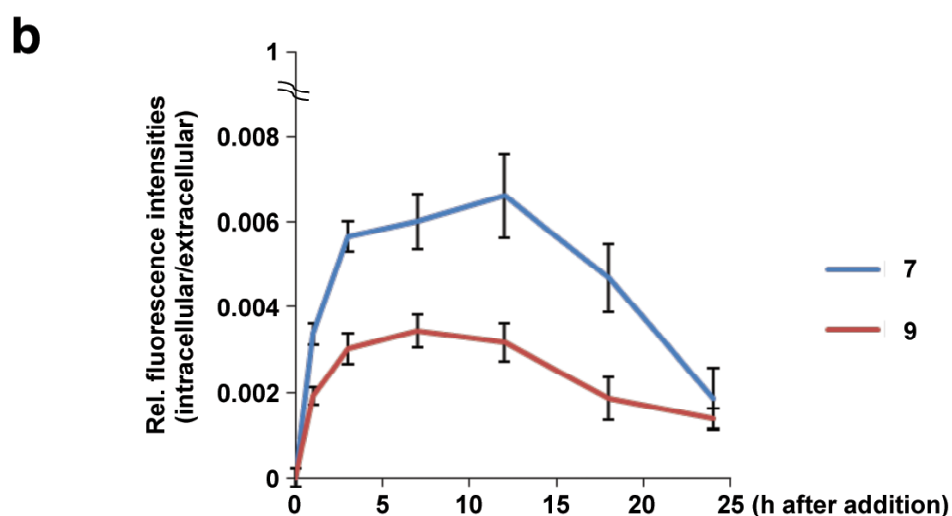
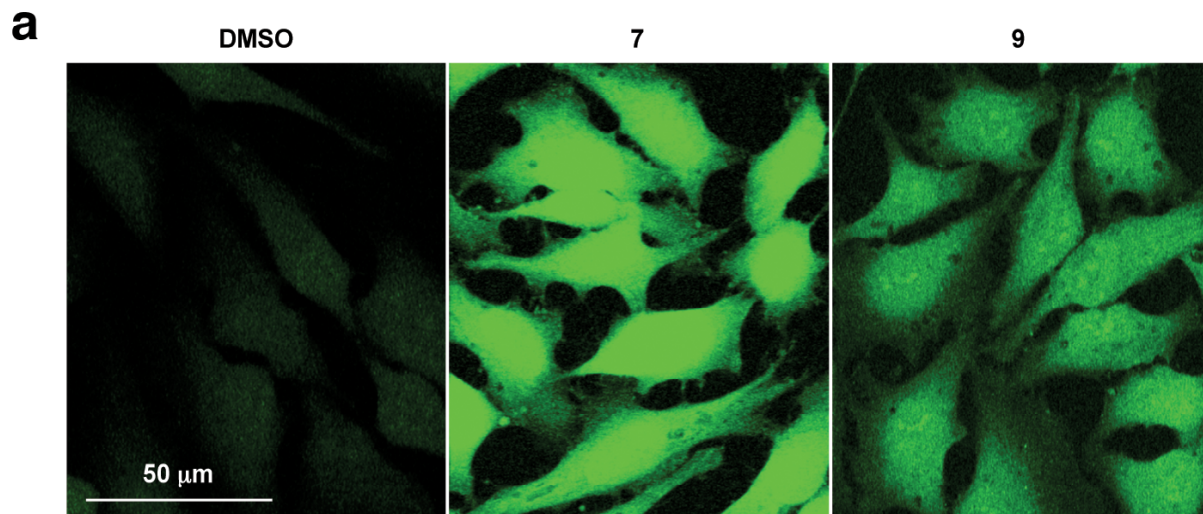




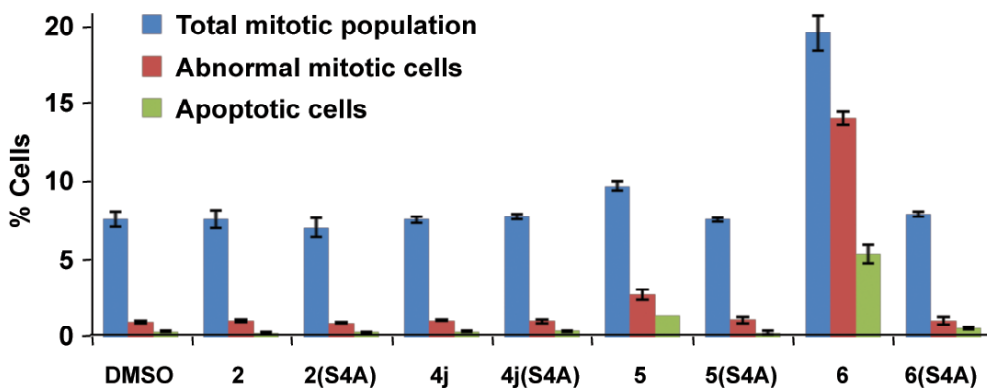
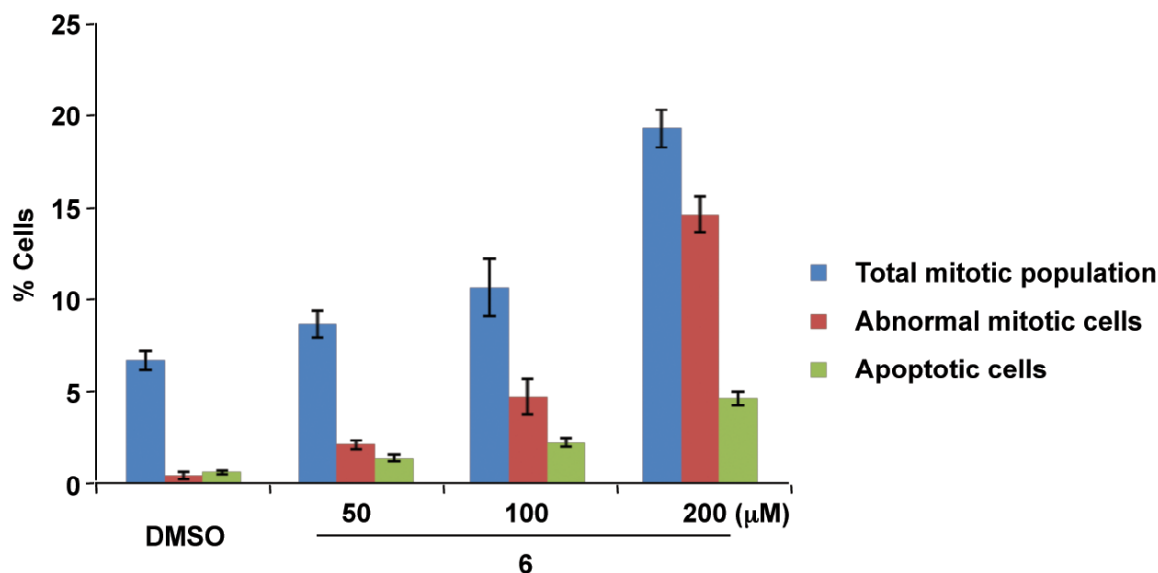
**Supplementary Figure 10:** Binding of fluorescein-labeled peptides to the PBDs of Plk1 (left column), Plk2 (center column), and Plk3 (right column) was analyzed by fluorescence polarization. Control peptides used were **14**(for Plk1 PBD), **15**(for Plk2 PBD), and **16** (for Plk3 PBD), respectively.



**Supplementary Figure 11.** Dose-dependent inhibition of cell proliferation by **6**. **(a-b)** HeLa cells were arrested in S phase by single thymidine treatment, released into fresh medium, and treated with various amounts of the indicated PEG conjugates 4 h after release. The cells were harvested at the 4, 10, 14, and 24 h time points after release for quantification **(a)**. The relative cell numbers for the indicated time points were determined in comparison to those of the respective 4 h samples. The  $\text{IC}_{50}$  of cell proliferation inhibition for **6** ( $\sim 380 \mu\text{M}$ ) was calculated using the data points from the 24 h samples. The transiently decreased cell numbers observed with  $800 \mu\text{M}$  of **6** at the 10 h and 14 h time points are likely due to cell death prior to cell doubling. Representative images of either untreated ( $0 \mu\text{M}$ , 4 h) or treated with the indicated concentrations of **6** for 24 h were provided **(b)**. Data in **(a)** represent mean values  $\pm$  s.d. obtained from three independent experiments.

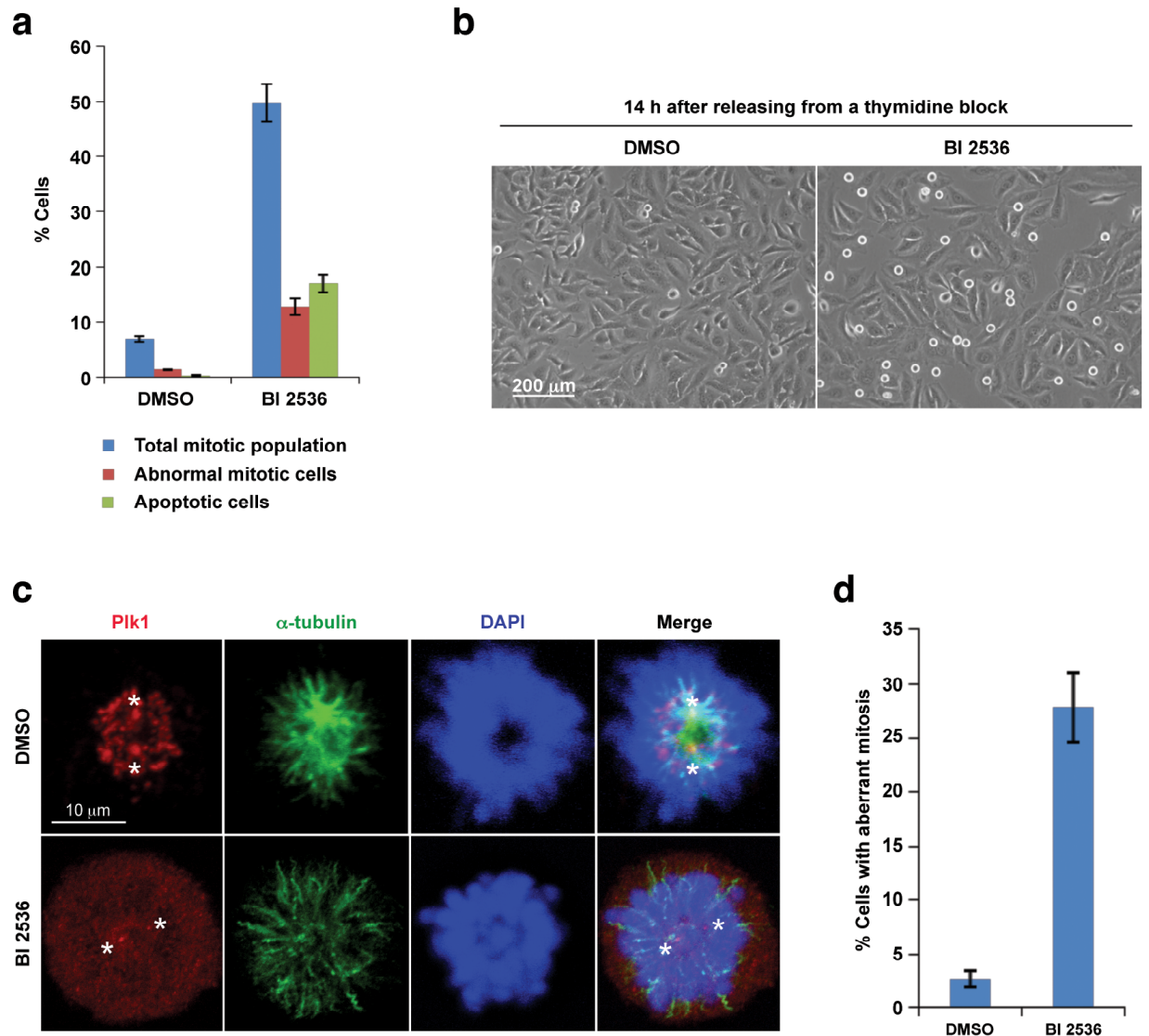


**Supplementary Figure 12.** Assessment of the membrane permeability of **6**. **(a)** HeLa cells grown on cover slips were treated with control DMSO or 200  $\mu\text{M}$  of either FITC-conjugated PEG or **9**. The cells were then harvested at the 0, 1, 3, 7, 12, 18, and 24 h time points after treatment, briefly dipped in PBS, and immediately fixed with 2% glutaraldehyde for 1 h at room temperature. The resulting samples were subjected to confocal microscopy for analyses. Represent images from the 7 h samples were shown. **(b)** From 20 randomly chosen cells at each time point, the entire intracellular fluorescent signals were quantified using Zeiss AIM confocal software after subtracting the background signal intensity from the DMSO-treated control cells. To determine the relative levels of internalized FITC conjugates, the total intracellular fluorescence signals were divided by the extracellular fluorescence signals obtained from the same area size of unwashed samples. Note that less than 0.4% of **9** was internalized during the first 7 h after treatment. The signal decrease at later time points could be in part due to the unstable nature of these conjugates *in vivo*. Data in **(b)** represent mean values  $\pm$  s.d. calculated from the average fluorescence intensities of 20 cells at each time point, obtained from each of three independent experiments.

**a****b**

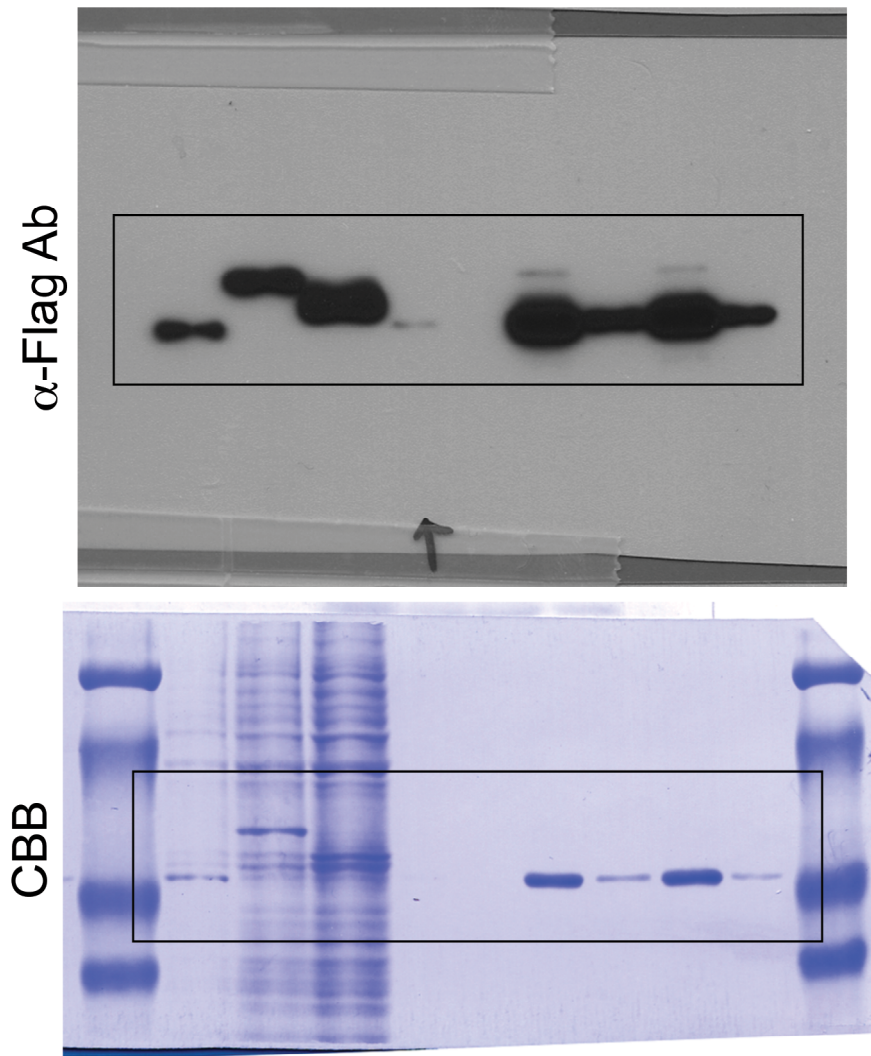
**Supplementary Figure 13.** Dose-dependent induction of mitotic arrest and apoptotic cell death by **6**. **(a)**, Asynchronously growing HeLa cells were treated with 200  $\mu\text{M}$  of the indicated compounds for 24 h (All the compounds were dissolved in DMSO because some of the non-PEGylated compounds were largely water-insoluble). The cells were additionally treated with Hoechst 33342 for 10 min, fixed with paraformaldehyde, and then quantified. Mean values  $\pm$  standard deviation (bars) were obtained from three independent experiments. **(b)**, Asynchronously growing HeLa cells were treated with the indicated concentrations of **6** [The PEGylated **6** compound was dissolved in phosphate-buffered saline (PBS)]. Twenty-four hours after treatment, the cells were prepared as in **(a)** and analyzed. Data represent mean values  $\pm$  standard deviation (bars) obtained from three independent experiments.





**Supplementary Figure 14.** Delayed induction of mitotic arrest and apoptotic cell death by the treatment of cells with BI 2536. **(a)** Asynchronously growing HeLa cells were treated with 100 nM of BI 2536, the concentration previously used to characterize its effect in cultured cells.<sup>14</sup> Twenty-four hours after treatment, the cells were stained with Hoechst 33342 for 10 min and analyzed as described in Supplementary **Fig. 13**. **(b)** HeLa cells were arrested with a single thymidine block and released into fresh medium. Four hours after release, cells were treated with either control DMSO or 100 nM of BI 2536. The resulting cells were then harvested at the 4, 6, 8, 10, 12, 14, 16, and 19 h time points after release to determine the percentage of mitotic cells with rounded-up morphology (See the result in **Fig. 2f**). The cells at the 14 h time point were photographed and representative images were provided. Note that cells treated with control DMSO reached mitosis 10 h after single thymidine release. However, cells treated with BI 2536 exhibited severely delayed cell cycle progression, but continuously accumulated mitotically round-up cells over time. **(c-d)** Cells released from a single thymidine block for 9 h were treated with BI 2536 for 2 h and then subjected to immunostaining analyses to examine Plk1 localization **(c)** and to quantify the cells with aberrant mitotic morphologies among the total mitotic population **(d)**. In good agreement with the previous observation,<sup>14</sup> treatment of cells with BI 2536 induced a

prometaphase arrest with drastically delocalized Plk1 signals from centrosomes (asterisks) and kinetochores, and greatly weakened spindle morphologies. Note that, as a result of delayed cell cycle progression by BI 2536 (see the results in **Fig. 2f**), the fraction of mitotically arrested cells in **(b)** and the percentage of aberrant mitotic cells in **(d)** were less than those from the **6**-treated cells in **Fig. 2c** and **Fig. 2e** of the published text. The results in **(a)** and **(d)** represent mean values  $\pm$  s.d. (bars) obtained from three independent experiments.



**Supplementary Figure 15.** The original images used to generate **Fig. 2a**.

## Supplementary Information References

1. Liu, F., Park, J.-E., Lee, K.S. & Burke, T.R. Preparation of orthogonally protected (2S,3R)-2-amino-3-methyl-4-phosphonobutyric acid (Pmab) as a phosphatase-stable phosphothreonine mimetic and its use in the synthesis of polo-box domain-binding peptides. *Tetrahedron* **65**, 9673-9679 (2009).
2. Yun, S.-M. et al. Structural and functional analyses of minimal phosphopeptides targeting the polo-box domain of polo-like kinase 1. *Nat. Struct. Mol. Biol.* **16**, 876-882 (2009).
3. Minor, W., Cymborowski, M., Otwinowski, Z. & Chruszcz, M. HKL-3000: the integration of data reduction and structure solution--from diffraction images to an initial model in minutes. *Acta Crystallogr. D Biol. Crystallogr.* **62**, 859-66 (2006).
4. The CCP4 suite: programs for protein crystallography. *Acta Crystallogr. D Biol. Crystallogr.* **50**, 760-3 (1994).
5. Navaza, J. Implementation of molecular replacement in AMoRe. *Acta Crystallogr. D Biol. Crystallogr.* **57**, 1367-72 (2001).
6. Adams, P.D. et al. PHENIX: a comprehensive Python-based system for macromolecular structure solution. *Acta Crystallogr. D Biol. Crystallogr.* **66**, 213-21.
7. McRee, D.E. XtalView/Xfit--A versatile program for manipulating atomic coordinates and electron density. *J. Struct. Biol.* **125**, 156-65 (1999).
8. Kraulis, P.J. MOLSCRIPT: A Program to Produce Both Detailed and Schematic Plots of Protein Structures. *J. Appl. Crystallogr.* **24**, 946-950 (1991).
9. Reindl, W., Strebhardt, K., and Berg, T. (2008). A high-throughput assay based on fluorescence polarization for inhibitors of the polo-box domain of polo-like kinase 1. *Anal. Biochem.* **383**, 205-209.
10. Reindl, W., Yuan, J., Krämer, A., Strebhardt, K., and Berg, T. (2008). Inhibition of Polo-like Kinase 1 by Blocking Polo-Box Domain-Dependent Protein-Protein Interactions. *Chem. Biol.* **15**, 459-466.
11. Reindl, W., Gräber, M., Strebhardt, K., and Berg, T. (2009). Development of high-throughput assays based on fluorescence polarization for inhibitors of the polo-box domains of polo-like kinases 2 and 3. *Anal. Biochem.* **395**, 189-194.
12. Reindl, W., Yuan, J., Krämer, A., Strebhardt, K., and Berg, T. (2009). A Pan-Specific Inhibitor of the Polo-Box Domains of Polo-like Kinases Arrests Cancer Cells in Mitosis. *Chembiochem* **10**, 1145-1148.
13. Seong, Y. S, et al. A spindle checkpoint arrest and a cytokinesis failure by the dominant-negative polo-box domain of Plk1 in U-2 OS cells. *J. Biol. Chem.* **277**, 32282-32293 (2002).
14. Lenart, P.; Petronczki, M.; Steegmaier, M.; Di Fiore, B.; Lipp, J. J.; Hoffmann, M.; Rettig, W. J.; Kraut, N.; Peters, J.-M. The small-molecule inhibitor BI 2536 reveals novel insights into mitotic roles of polo-like kinase 1. *Curr. Biol.* **2007**, *17*, 304-315.